



HAL
open science

High performance dyes based on triphenylamine, cinnamaldehyde and indane-1,3-dione derivatives for blue light induced polymerization for 3D printing and photocomposites

Mira Abdallah, Frederic Dumur, Bernadette Graff, Akram Hijazi, Jacques Lalevee

► To cite this version:

Mira Abdallah, Frederic Dumur, Bernadette Graff, Akram Hijazi, Jacques Lalevee. High performance dyes based on triphenylamine, cinnamaldehyde and indane-1,3-dione derivatives for blue light induced polymerization for 3D printing and photocomposites. *Dyes and Pigments*, 2020, pp.108580. 10.1016/j.dyepig.2020.108580 . hal-02906497

HAL Id: hal-02906497

<https://hal.science/hal-02906497v1>

Submitted on 24 Jul 2020

HAL is a multi-disciplinary open access archive for the deposit and dissemination of scientific research documents, whether they are published or not. The documents may come from teaching and research institutions in France or abroad, or from public or private research centers.

L'archive ouverte pluridisciplinaire **HAL**, est destinée au dépôt et à la diffusion de documents scientifiques de niveau recherche, publiés ou non, émanant des établissements d'enseignement et de recherche français ou étrangers, des laboratoires publics ou privés.

High Performance Dyes Based on Triphenylamine, Cinnamaldehyde and Indane-1,3-dione Derivatives for Blue Light Induced Polymerization for 3D Printing and Photocomposites

Mira Abdallah,^{1,2,3} Frédéric Dumur,⁴ Bernadette Graff^{1,2}, Akram Hijazi,³ Jacques Lalevée*^{1,2}

¹Université de Haute-Alsace, CNRS, IS2M UMR 7361, F-68100 Mulhouse, France

²Université de Strasbourg, France

³EDST, Université Libanaise, Campus Hariri, Hadath, Beyrouth, Liban

⁴Aix Marseille Univ, CNRS, ICR UMR 7273, F-13397 Marseille, France

Corresponding author: jacques.lalevee@uha.fr

ABSTRACT:

In this research, high performance dyes based on triphenylamine, cinnamaldehyde and indane-1,3-dione derivatives have been designed/synthesized and evaluated as photoinitiators for visible light photopolymerization. The introduction of light-emitting diodes (LEDs) as low-cost and **secured** sources of irradiation is one of the major purposes in this study, where a LED at 405 nm was used for both the cationic polymerization (CP) of thin epoxide samples and the free radical polymerization (FRP) of thin TMPTA films. The proposed dyes showed very high efficiencies in the presence of the two-component photoinitiating systems based on Dye/Iodonium salt (Iod) couples or Dye/Amine (such as *N*-Phenylglycine (NPG) or ethyl 4-(dimethylamino)benzoate (EDB)) couples for the FRP and/or CP, highlighting their importance through a photo-oxidation (with Iod) process but also through a photo-reduction (with amine) process. The examined dyes are also able to initiate the FRP of thin acrylate films in the presence of the three-component (Dye/Iod/NPG) systems where very high rates of polymerization (R_p) and great final reactive function conversions (FCs) were achieved. Objectives of this work concern the study of the photoinitiating abilities of the different photoinitiating systems using FTIR technique but also the

study of the chemical mechanisms which was mainly examined in solution. The use of the investigated systems for 3D printing experiments (using LED projector or laser diode @405 nm) is particularly outlined. Finally, the production of thick glass fiber photocomposites presenting excellent depth of cure is also accomplished in the presence of these dyes (using near-UV conveyor: LED@395 nm).

KEYWORDS: Dyes; Free Radical Polymerization; Photoinitiator; Photopolymerization; 3D printing resin.

1. INTRODUCTION

During the past decades, a great deal of efforts has been devoted to develop new manufacturing processes allowing to produce polymers in safer but also in more ecological conditions. To fulfill this last requirement, light and more precisely visible light has rapidly been identified as a cheap and easy-to-handle energy source for the manufacture of polymers. A general overview of the different polymerization processes induced by light is reported in [1]. These latter are characterized by several economic advantages compared to heat induced processes and some of the most important characteristics can be cited: low energy consumption, use of low polymerization temperatures, low emission of volatile organic compounds, low operating costs [2-16], spatial control of the process and so on.

One of the major challenges in light-curing processes is the use of visible light emitted by light-emitting diodes (LEDs) and displaying very low intensities [3,8-16]. Hence, comes the need to develop new photoinitiating systems capable to generate highly reactive initiating species to initiate the photopolymerization processes under visible light.

Several examples of dyes which are able to initiate polymerization processes upon visible light irradiation are reported in literature including as examples: naphthalimide and naphthalic anhydride derivatives (blue light sensitive dyes) for cationic, radical and thiol-ene photopolymerizations [17], methylene blue-triethanolamine for aqueous acrylamide photopolymerization [18], dihydroxyanthraquinone derivatives (natural dyes as blue-light-sensitive versatile photoinitiators for free radical and cationic photopolymerization [19]), indanedione derivatives for radical, cationic and thiol-ene photopolymerization reactions [20,21], D-D-A dyes with phenothiazine-carbazole/triphenylamine as double donors for the cationic polymerization of bisphenol-A epoxy resin A (DGEBA) and the free radical polymerization of tripropylene glycol diacrylate (TPGDA) under 455 nm and 532 nm laser beams [22], triphenylamine-hexaarylbiimidazole derivatives as hydrogen-acceptor photoinitiators for free radical photopolymerization under UV and LED light [23], photopolymerization of acrylate suspensions with visible dyes [24], and so on. Otherwise, the role of dyes in the photoinitiation processes of polymerization reactions is also presented in e.g. [25].

In this work, high performance dyes based on triphenylamine, cinnamaldehyde and indane-1,3-dione derivatives are designed/synthesized and investigated as photoinitiators for the free radical polymerization of thin acrylate films and the cationic polymerization of thin epoxide samples upon irradiation with a LED at 405 nm. In order to generate reactive initiating species, the investigated dyes are incorporated into two-component photoinitiating systems based on Dye/Iod (or NPG or EDB) couples but also into three-component PISs based on Dye/Iod/NPG combinations.

Using different techniques such as UV-visible spectroscopy, cyclic voltammetry, fluorimetry and electron spin resonance (ESR), a global photochemical mechanism explaining the

interactions which can take place in the excited states is proposed. The generation of thick 3D patterns was also possible in the presence of the examined dyes using 3D printing experiments. Moreover, the preparation of thick glass fiber photocomposites was fruitfully achieved in the presence of the involved dyes, using a near-UV conveyor (LED at 395 nm).

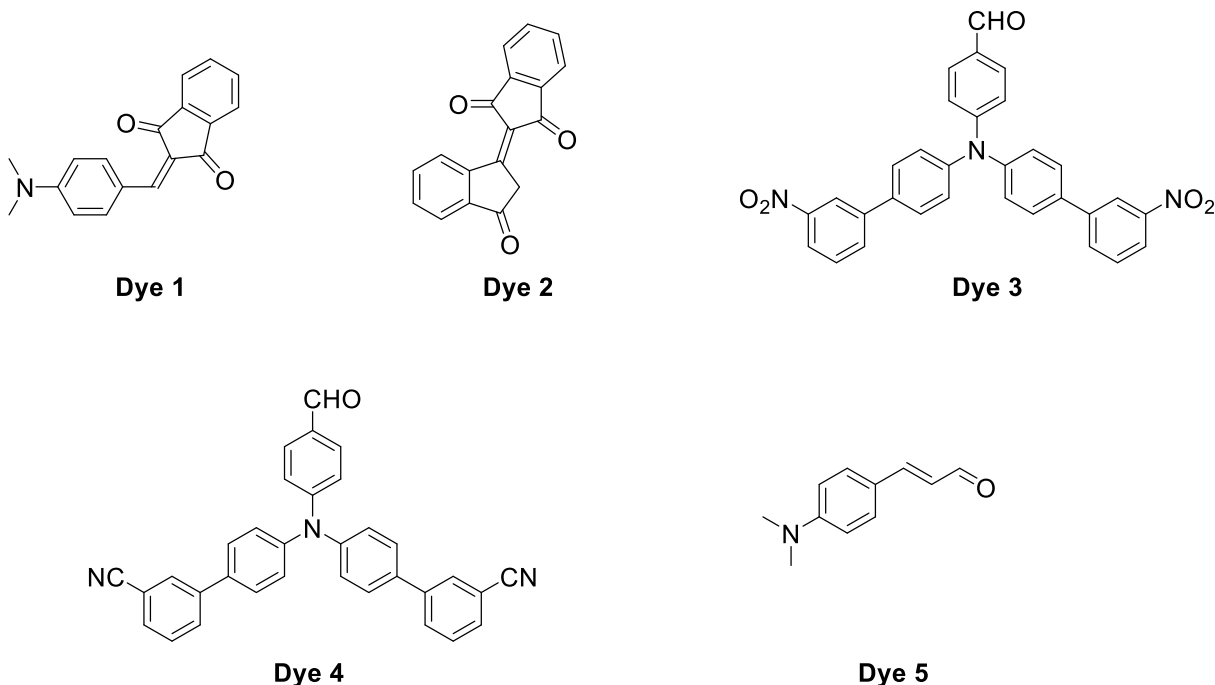


Figure 1. Chemical Structures of the Different Dyes used in this Research.

2. EXPERIMENTAL PART

2.1. Synthesis of the Investigated Dyes

All details concerning the ^1H and ^{13}C NMR, HMRS and elemental analyses, the different suppliers for chemicals have been fully detailed in our previous works.[26] **Dye 1** [27], **Dye 2** [28] and **Dye 5** [29] and 4-(bis(4-bromophenyl)amino)benzaldehyde [30] were synthesized as previously reported in the literature, without modifications and in similar yields.

Synthesis of 4-(bis(3'-nitro-[1,1'-biphenyl]-4-yl)amino)benzaldehyde (Dye 3)

Tetrakis(triphenylphosphine)palladium (0) (0.46 g, 0.744 mmol, $M = 1155.56 \text{ g}\cdot\text{mol}^{-1}$) was added to a mixture of 4-(bis(4-bromophenyl)amino)benzaldehyde (2.52 g, 6.11 mmol, $M = 413.13 \text{ g}\cdot\text{mol}^{-1}$), (3-nitrophenyl)boronic acid (2.11 g, 12.66 mmol, $M = 166.93 \text{ g}\cdot\text{mol}^{-1}$), toluene (54 mL), ethanol (26 mL) and an aqueous potassium carbonate solution (2 M, 6.91 g in 25 mL water, 26 mL) under vigorous stirring. The mixture was stirred at 80 °C for 48 h under a nitrogen atmosphere. After cooling to room temperature, the reaction mixture was poured into water and extracted with ethyl acetate. The organic layer was washed with brine several times, and the solvent was then evaporated. Addition of DCM followed by pentane precipitated a white solid which was filtered off. The residue was purified by column chromatography (SiO_2 , pentane/DCM: 1/1 and pure DCM) and isolated as a solid (2.78 g, 88% yield). ^1H NMR (CDCl_3) δ : 7.20 (d, 2H, $J = 8.7 \text{ Hz}$), 7.32 (d, 4H, $J = 8.6 \text{ Hz}$), 7.61-7.65 (m, 6H), 7.78 (d, 2H, $J = 8.7 \text{ Hz}$), 7.91-7.94 (m, 2H), 8.19-8.22 (m, 2H), 8.46 (t, 2H, $J = 1.9 \text{ Hz}$), 9.89 (s, 1H); ^1H NMR (DMSO-d_6) δ : 7.11 (d, 2H, $J = 8.6 \text{ Hz}$), 7.31 (d, 4H, $J = 8.5 \text{ Hz}$), 7.73-7.86 (m, 8H), 8.15-8.22 (m, 4H), 8.44 (s, 2H), 9.85 (s, 1H); ^{13}C NMR (DMSO-d_6) δ : 120.3, 120.7, 121.9, 126.2, 128.5, 129.8, 130.5, 131.3, 132.9, 134.2, 140.8, 145.9, 148.4, 152.0, 190.8; HRMS (ESI MS) m/z : theor: 516.1554 found: 516.1556 [$\text{M}+\text{H}$] $^+$ detected). Analyses were consistent with those previously reported in the literature [31]

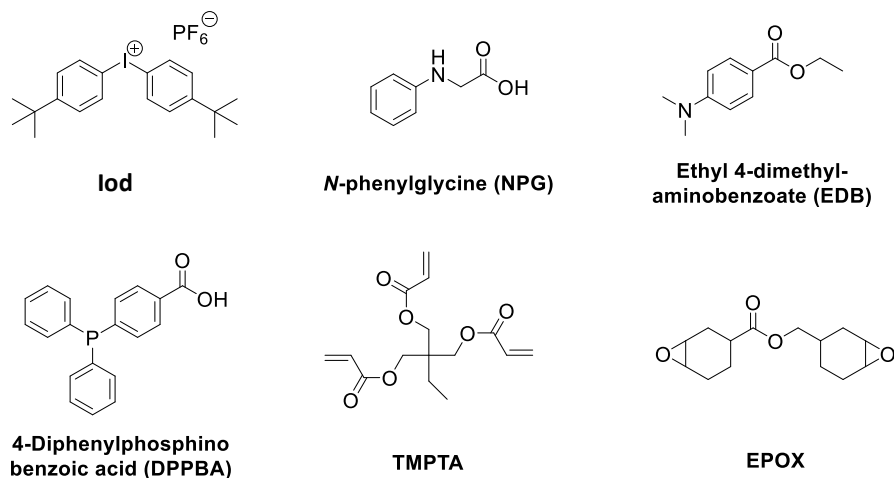
Synthesis of 4',4'''-((4-formylphenyl)azanediyl)bis((1,1'-biphenyl)-3-carbonitrile) (Dye 4)

Tetrakis(triphenylphosphine)palladium (0) (0.46 g, 0.744 mmol, $M = 1155.56 \text{ g}\cdot\text{mol}^{-1}$) was added to a mixture of 4-(bis(4-bromophenyl)amino)benzaldehyde (2.52 g, 6.11 mmol, $M = 413.13 \text{ g}\cdot\text{mol}^{-1}$), (3-cyanophenyl)boronic acid (1.86 g, 12.66 mmol, $M = 146.94 \text{ g}\cdot\text{mol}^{-1}$), toluene (54 mL), ethanol (26 mL) and an aqueous potassium carbonate solution (2 M, 6.91 g in 25 mL water, 26 mL) under vigorous stirring. The mixture was stirred at 80 °C for 48 h under a nitrogen atmosphere. After cooling to room temperature, the reaction mixture was poured into water and extracted with

ethyl acetate. The organic layer was washed with brine several times, and the solvent was then evaporated. Addition of DCM followed by pentane precipitated a white solid which was filtered off. The residue was purified by column chromatography (SiO₂, pentane/DCM: 1/1 and pure DCM) and isolated as a solid (2.38 g, 82% yield). ¹H NMR (DMSO-d₆) δ : 7.06-7.11 (m, 2H), 7.22-7.32 (m, 4H), 7.55-7.84 (m, 12H), 8.04 (d, 1H, J = 7.7 Hz), 8.17 (s, 1H), 9.84 (s, 1H); Anal. Calc. for C₃₃H₂₁N₃O : C, 83.3; H, 4.4; O, 3.4; Found: C, 83.4; H, 4.6; O, 3.5 %; HRMS (ESI MS) m/z: theor: 476.1757 found: 476.1754 [M+H]⁺ detected).

2.2. Other Chemicals

All commercial chemicals were selected with the highest purity available and used as received. Their chemical structures are presented in the Scheme 1. *Bis(4-tert-butylphenyl)iodonium hexafluorophosphate* (Iod or SpeedCure 938) was obtained from Lambson Ltd (UK). *N*-Phenylglycine (NPG), ethyl 4-(dimethylamino)benzoate (EDB) and 4-(diphenylphosphino)benzoic acid (DPPBA) were obtained from Sigma Aldrich. (3,4-Epoxy cyclohexane)methyl 3,4-epoxycyclohexylcarboxylate (EPOX; Uvacure 1500) and trimethylolpropane triacrylate (TMPTA) were obtained from Allnex. TMPTA and EPOX were selected as benchmark monomers for radical and cationic polymerization, respectively.



Scheme 1. Chemicals used as Additives and Monomers for this Study.

2.3. Near-UV and Visible Light Irradiation Sources

The two following **Light-Emitting** Diodes (LEDs) were used **as the** light irradiation sources for this study: (i) LED@375 nm; incident light intensity at the sample surface: $I_0 = 40 \text{ mW. cm}^{-2}$ for the steady state photolysis experiments, and (ii) LED@405nm ($I_0 = 110 \text{ mW. cm}^{-2}$) for the photopolymerization processes which are followed by (RT)-FTIR.

2.4. Cationic Photopolymerization (CP) and Free Radical Photopolymerization (FRP) followed by Real-Time (RT)-FTIR

In this work, Dye/Iod (or NPG or EDB) (0.5%/1% w/w) have been used as two-component photoinitiating systems (PISs) for the FRP and/or CP. In addition, dyes have been also incorporated into three-component Dye/Iod/NPG (0.5%/1%/1% w/w) PISs for the FRP. The weight percent of the different chemical compounds included in the photoinitiating systems is calculated from the monomer content (w/w). A BaF₂ pellet is used for the CP of thin EPOX samples where the photosensitive formulation (thickness ~25 μm, under air) is put on it. Conversely, propylene films are used for the FRP of thin TMTPA samples where the photosensitive formulation is sandwiched between two propylene films (in laminate) in order to reduce oxygen inhibition. Evolution of the characteristic peak of the epoxy group content of EPOX and the double bond content of acrylate functions was continuously followed by real time (RT)-FTIR spectroscopy (JASCO FTIR 4100) at about 790 and 1630cm⁻¹, respectively. The procedure followed to monitor the photopolymerization profiles has been already described in detail in [32,33,34].

2.5. Cyclic Voltammetry for the Access to Redox Potentials

Cyclic voltammetry experiments have been carried out in order to determine the redox potentials (E_{ox} and E_{red}) of the different dyes used in this research. These experiments were performed in acetonitrile and in the presence of tetrabutylammonium hexafluorophosphate (0.1 M) as the supporting electrolyte (potential vs. Saturated Calomel Electrode - SCE). Then, the free energy change (ΔG_{et}) for the electron transfer reaction was calculated according to equation 1 (eq 1) [35], where E_{ox} , E_{red} and E^* stand for the oxidation potential of the electron donor, the reduction potential of the electron acceptor and the excited state energy (E_{S1} or E_{T1}), respectively. C is the coulombic term for the initially formed ion pair which is usually neglected in polar solvents.

$$\Delta G_{et} = E_{ox} - E_{red} - E^* + C \quad (\text{eq 1})$$

2.6. ESR Spin-Trapping (ESR-ST) Experiments

Tert-butylbenzene was chosen as the solvent for the ESR-ST experiments which are performed using an X-Band spectrometer (Magnettech MS400). A LED@405 nm was used as a source of irradiation in order to trigger the generation of radicals under N_2 at room temperature (RT). Following a procedure described elsewhere in detail in [33,34], phenyl-*N-tert*-butylnitronone (PBN) has been added to the medium in order to trap the generated radicals. The ESR spectra simulations are obtained from the PEST WINSIM program.

2.7. UV-Visible Absorption and Photolysis Experiments

Absorption properties of the different dyes used in this work as well as the steady state photolysis experiments were studied using a JASCO V730 UV-visible spectrometer.

2.8. Fluorescence and Fluorescence Quenching Experiments

A JASCO FP-6200 spectrofluorimeter was used in order to study the fluorescence properties as well as the fluorescence quenching data of the examined compounds.

2.9. Computational Procedure

The frontier orbitals (HOMO and LUMO) as well as the UV-Visible spectra of the different investigated dyes were calculated at Density Functional Theory (DFT) level (UB3LYP/6-31G*). The triplet state energy was evaluated after full geometry optimization of both S_0 and T_1 . The computational procedure was described by us in [36].

2.10. 3D Printing Experiments using Laser Diode or LED Projector

A laser diode @405 nm (spot size of 50 μm) or a LED projector at 405 nm were used as the light irradiation sources for 3D printing experiments which were performed under air. Various thicknesses were obtained for the generated 3D patterns. These latter were analyzed by a numerical optical microscopy (DSX-HRSU from OLYMPUS Corporation) as reported by us in [37,38].

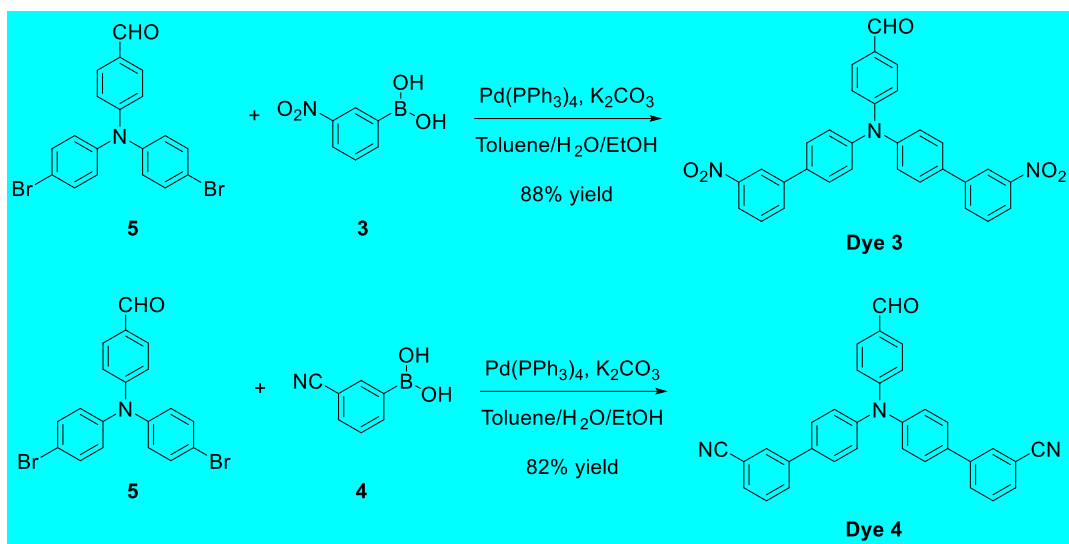
2.11. Near-UV Conveyor using LED at 395 nm

The production of photocomposites was carried out using a Dymax near-UV conveyor which is equipped with a 120 mm wide Teflon-coated belt (the belt speed was fixed at 2 m. min^{-1}). A LED @395 nm (4W/cm²) was used to cure the impregnated glass fibers/organic resin (50%/50% w/w) composites.

3. RESULTS AND DISCUSSION

3.1. Dyes Synthesis

Due to the diversity of structures reported in this work, the five dyes were synthesized using a specific synthetic approach (Scheme 2). Thus, to produce **Dye 1**, a Knoevenagel reaction involving the reflux of an equimolar amount of 4-dimethylaminobenzaldehyde **1** and indane-1,3-dione **2** in ethanol in the presence of a few drops of piperidine was performed. **Dye 1** could be obtained with a reaction yield of 80%, consistent with those reported in the literature [27]. Concerning **Dye 2**, several strategies can be used to prepare this strong electron acceptor [1,2'-biindenylidene]-1',3,3'(2*H*)-trione also named "bindone". Notably, self-condensation of indane-1,3-dione in weakly basic conditions is often observed as a major drawback during the synthesis of indane-1,3-dione-based push-pull dyes. In the present case, use of sodium acetate as the base was enough to self-condense indane-1,3-dione **2** at room temperature for one hour and furnish after hydrolysis **Dye 2** in 66% yield [28]. **Dye 3** and **Dye 4** could be prepared using a similar synthetic route involving a Suzuki cross-coupling reaction of (3-nitrophenyl)boronic acid **3** and (3-cyanophenyl)boronic acid **4** respectively with 4-(bis(4-bromophenyl)amino)benzaldehyde **5** using tetrakis(triphenylphosphine)palladium (0) as the catalyst and potassium carbonate as the base. The two dyes **Dye 3** and **Dye 4** could be prepared in 88 and 82% yields respectively (See Scheme 2). Finally, **Dye 5** was obtained in a single step procedure consisting in an acid-catalyzed aldol condensation of acetaldehyde **6** on 4-dimethylaminobenzaldehyde **1**. **Dye 5** could be obtained in 65% yield, higher than that reported in the literature. [29] Enhancement of the reaction yield was notably obtained by using an excess of acetaldehyde, this latter being highly volatile (boiling point \div 20°C).



Scheme 2. Synthetic routes to **Dye 1-Dye 5**.

3.2. Light Absorption Properties of the Investigated Dyes

The UV-Visible absorption experiments were carried out in acetonitrile. The investigated dyes present very high molar extinction coefficients in the near-UV and blue region providing a very good overlap with the emission spectra of the near-UV or visible light irradiation sources used in this study (LED@375 or @405 nm) e.g. $\epsilon(\text{Dye 1}) = 40330 \text{ M}^{-1} \cdot \text{cm}^{-1}$ at $\lambda_{\text{max}} = 479 \text{ nm}$, $\epsilon(\text{Dye 3}) = 26610 \text{ M}^{-1} \cdot \text{cm}^{-1}$ at $\lambda_{\text{max}} = 352 \text{ nm}$. The absorption spectra of the investigated dyes are presented in Figure 2 and the light absorption parameters are gathered in Table 1.

The optimized geometries as well as the frontier orbitals (Highest Occupied Molecular Orbital (HOMO) and Lowest Unoccupied Molecular Orbital (LUMO)) for the examined dyes are given in Figure 3. HOMOs and LUMOs are highly delocalized all over the π -conjugated systems resulting in low $\pi \rightarrow \pi^*$ transition energies. On the opposite, a partial charge transfer transition character is observed for **Dye 3** with a LUMO energy level localized on a single part of the molecule.

Figure 2. UV-Visible absorption spectra for the investigated dyes in acetonitrile: (1) **Dye 1**; (2) **Dye 3**; (3) **Dye 4**; and (4) **Dye 5**.

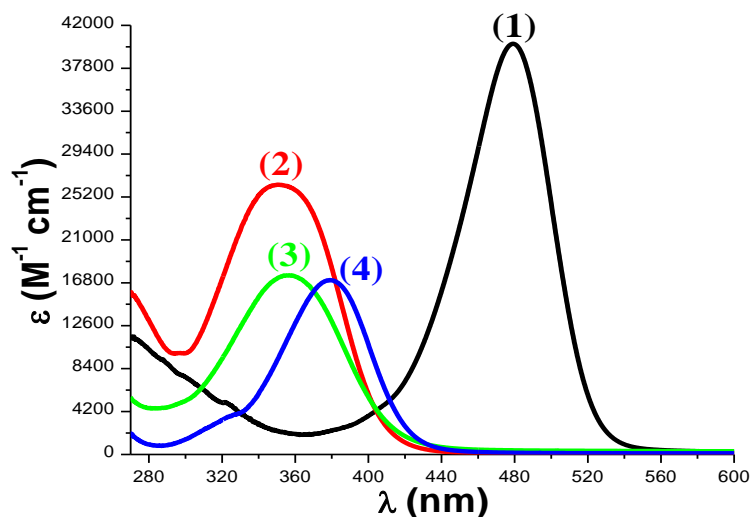
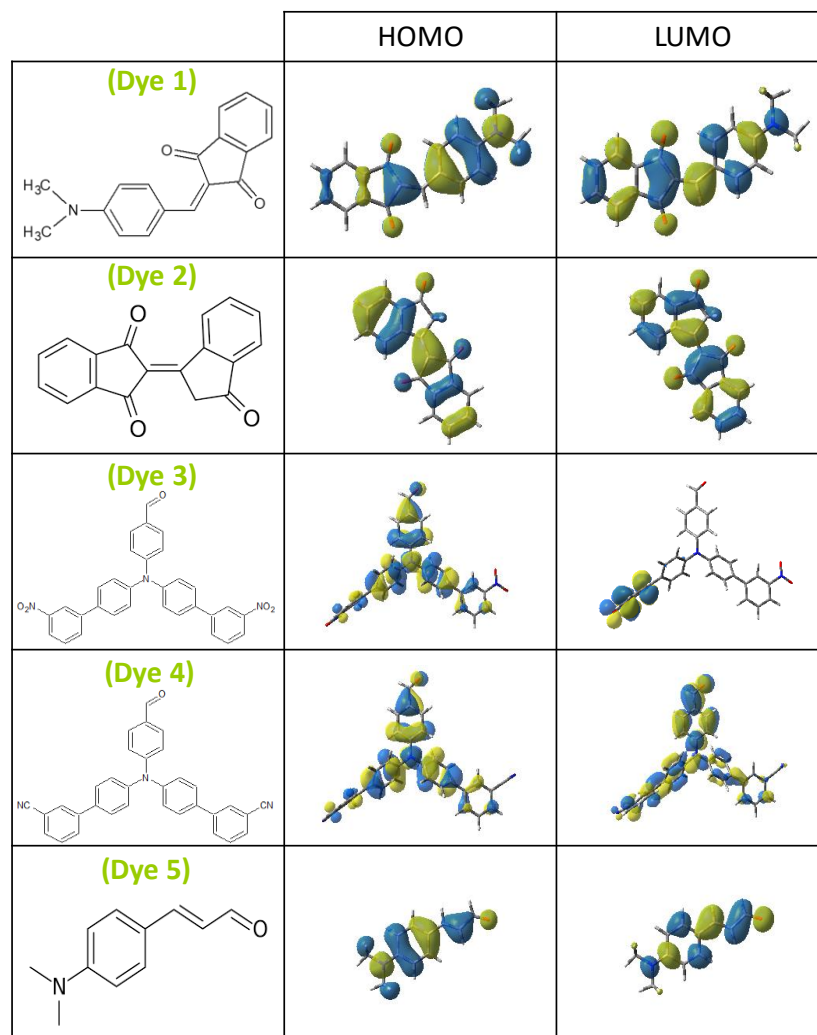


Table 1. The Light Absorption Parameters of the Investigated Dyes: Maximum Absorption Wavelengths (λ_{max}), Extinction Coefficients at λ_{max} (ϵ_{max}) and Extinction Coefficients at the Emission Wavelength of the LED@405 nm ($\epsilon_{@405\text{nm}}$).

PI	λ_{max} (nm)	ϵ_{max} ($M^{-1} \cdot \text{cm}^{-1}$)	$\epsilon_{@405\text{nm}}$ ($M^{-1} \cdot \text{cm}^{-1}$)
Dye 1	479	40330	4400
Dye 3	352	26610	4110
Dye 4	357	17700	4740
Dye 5	380	17250	8620

Figure 3. Contour Plots of HOMOs and LUMOs for the Dyes; Structures Optimized at the B3LYP/6-31G* Level of Theory.



3.3. Cationic Polymerization (CP) of Epoxides (EPOX)

The CP of thin epoxides samples (25 μm) was carried out under air, and upon irradiation with the LED at 405 nm (Figure 4). Generally, the investigated dyes (with the exception of Dye 2) are very efficient to initiate the CP when they are incorporated into two-component photoinitiating systems in the presence of an iodonium salt as the additive (Dye/Iod (0.5%/1% w/w)), promoting the polymerization through a photo-oxidation process e.g. final epoxy function conversion (FC) = 57% for Dye 4 (curve 4 in Figure 4A; Table 2). A new characteristic peak that corresponds to the formation of the polyether network appears at $\sim 1080\text{ cm}^{-1}$ in the FTIR spectra during the

photopolymerization (see Figure 4B). Actually, Iod or Dyes alone show no polymerization, highlighting the huge role of the dye in the system.

When comparing the polymerization profiles, the efficiency trend for CP (i.e. for the Rp) follows the order: **Dye 4 > Dye 5 > Dye 3 > Dye 1 >>> Dye 2**. Currently, this behavior is linked to the light absorption properties ($\epsilon_{@405\text{ nm}}$) of these dyes, their free energy changes of the electron transfer (ΔG_{et}) with iodonium but also their electron transfer quantum yields (ϕ_{et}) in the presence of Iod (see below the chemical **mechanism**). This suggests that both the light absorption properties but also the photochemical reactivity govern the dye efficiency. Otherwise, the reactivity of the generated radical cations ($\text{Dye}^{\bullet+}$) can significantly affect the initiating abilities of the involved systems (see the chemical mechanisms below). In addition, the formation of Brønsted acid as initiating species [39] can also influence the reactivity of the system.

Figure 4. (A) Polymerization profiles (epoxy function conversion vs irradiation time) of thin epoxide films (25 μm) under air upon irradiation with the LED@405 nm, in the presence of the two-component photoinitiating systems based on **Dye/Iod** (0.5%/1% w/w) couples: (1) **Dye 1/Iod**; (2) **Dye 2/Iod**; (3) **Dye 3/Iod**; (4) **Dye 4/Iod**; and (5) **Dye 5/Iod**. The irradiation starts at $t = 10\text{ s}$. (B) IR spectra recorded before and after polymerization of epoxide film, in the presence of **Dye 4/Iod** (0.5%/1% w/w) when irradiated with the LED@405 nm.

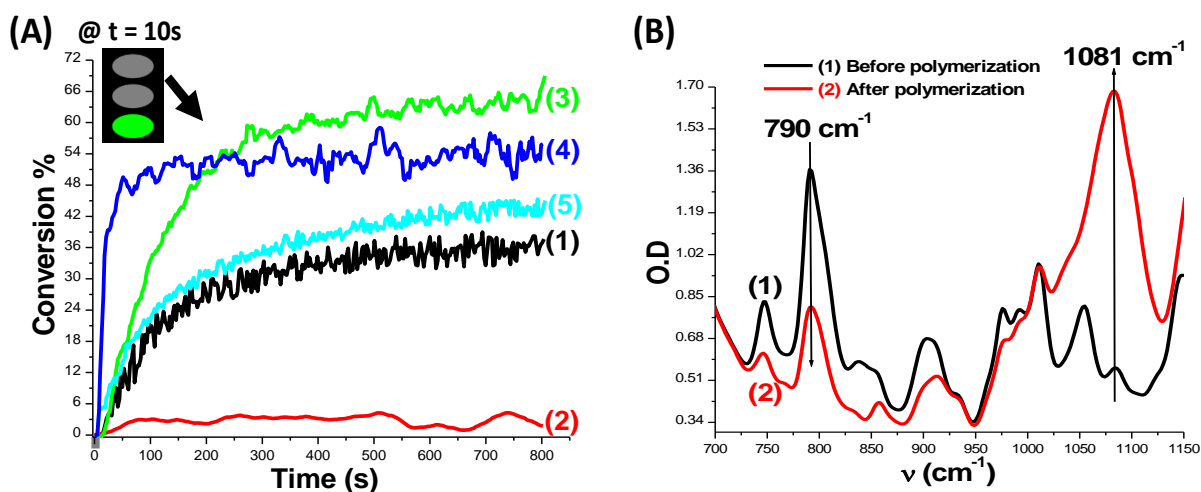


Table 2. Final Reactive Epoxy Function Conversion (FC) for EPOX in the Presence of Different Two-Component Photoinitiating Systems after 800s (LED @405 nm).

Dye/Iod (0.5%/1% w/w) (thickness = 25 μm) under air				
Dye 1/Iod	Dye 2/Iod	Dye 3/Iod	Dye 4/Iod	Dye 5/Iod
39%	n.p.	66%	57%	46%

n.p.: no polymerization

3.4. Free Radical Polymerization of Acrylates (TMPTA)

Very high efficiencies were shown for the free radical polymerization (FRP) of TMPTA in thin films, in the presence of the different two or three-component PISs (Dye/Iod, Dye/NPG, Dye/EDB or Dye/Iod/NPG). The FRP experiments were done in laminate and upon irradiation with the LED @405 (Figure 5; Table 3). Both high final acrylate function conversions (FCs) and rates of polymerization (R_p) were achieved in the presence of these dyes. As expected, dyes, Iod, NPG or EDB alone are not able to initiate the free radical polymerization of acrylates under the same irradiation conditions.

As shown in Figure 5A, **Dye 5** is the most efficient photoinitiator among this series to initiate the FRP of TMPTA through a photo-oxidation process in the presence of the Iodonium salt as an additive (curve 5 vs. curves 1-4 for the other dyes). This can be related to the highest extinction coefficient @405 nm of **Dye 5** compared to the other dyes ($\epsilon_{(405\text{ nm})} = 8620\text{ M}^{-1}\cdot\text{cm}^{-1}$ for **Dye 5** compared to $910\text{ M}^{-1}\cdot\text{cm}^{-1}$ for **Dye 2**, and so on; see in Table 1). The efficiency trend for FRP (i.e. for the R_p) follows the following order: **Dye 5** > **Dye 4** > **Dye 1** > **Dye 3** > **Dye 2** which nicely fit with the light absorption properties of these dyes.

Besides, good polymerization profiles were obtained for the FRP of thin TMPTA films in the presence of (Dye/NPG) couples, which occurs through a photo-reduction process (Figure 5B). The efficiency trend for (Dye/NPG) couples (i.e. for the R_p) follows the order: **Dye 4 > Dye 5 > Dye 3 > Dye 2 > Dye 1**. This trend is connected to two parameters which are the extinction coefficients ($\epsilon_{@405\text{ nm}}$) of these compounds and their free energy changes of the electron transfer (ΔG_{et}) with amine (see below for the chemical mechanisms). The electron transfer quantum yield (ϕ_{et}) is not able to explain the reactivity of the dyes in the presence of amines due to the fact that there is perhaps a back electron transfer which is illustrated by a non or poor photolysis (see the section 3.7.1. in the chemical mechanisms part).

Furthermore, when NPG is replaced by another amine (EDB), the investigated dyes **showed** also good initiating abilities (Figure 5D). In addition, a difference of order in the trend of efficiency is noticed between (Dye/NPG) and (Dye/EDB) couples. This may be related to the back electron transfer phenomenon.

Regarding the three-component (Dye/Iod/NPG) systems, a clear increase of the performance is noticed when NPG was added compared to the two-component (Dye/Iod) systems i.e. higher FCs and R_p s are obtained (Figure 5C vs. Figure 5A). In addition, a very low polymerization ability was shown in the presence of the two-component Iod/NPG (1%/1% w/w) system (curve 6 in Figure 5C), showing again the huge effect of the investigated dyes for the global performance of the systems.

Figure 5. Polymerization profiles (acrylate function conversion vs. irradiation time) of thin TMPTA films (25 μm , in laminate, using LED@405 nm), in the presence of different two and three-component photoinitiating systems: **(A) Dye/Iod (0.5%/1% w/w):** (1) Dye 1/Iod; (2) Dye 2/Iod; (3) Dye 3/Iod; (4) Dye 4/Iod; and (5) Dye 5/Iod. **(B): Dye/NPG (0.5%/1% w/w):** (1) Dye 1/NPG; (2) Dye 2/NPG; (3) Dye 3/NPG; (4) Dye 4/NPG; and (5) Dye 5/NPG. **(C) Dye/Iod/NPG (0.5%/1%/1% w/w):** (1) Dye 1/Iod/NPG; (2) Dye 2/Iod/NPG; (3) Dye 3/Iod/NPG; (4) Dye 4/Iod/NPG; (5) Dye 5/Iod/NPG; and (6) Iod/NPG (1%/1% w/w). **(D) Dye/EDB (0.5%/1% w/w):**

(1) Dye 1/EDB; (2) Dye 2/EDB; (3) Dye 3/EDB; (4) Dye 4/EDB; and (5) Dye 5/EDB. The irradiation starts for $t = 8$ s.

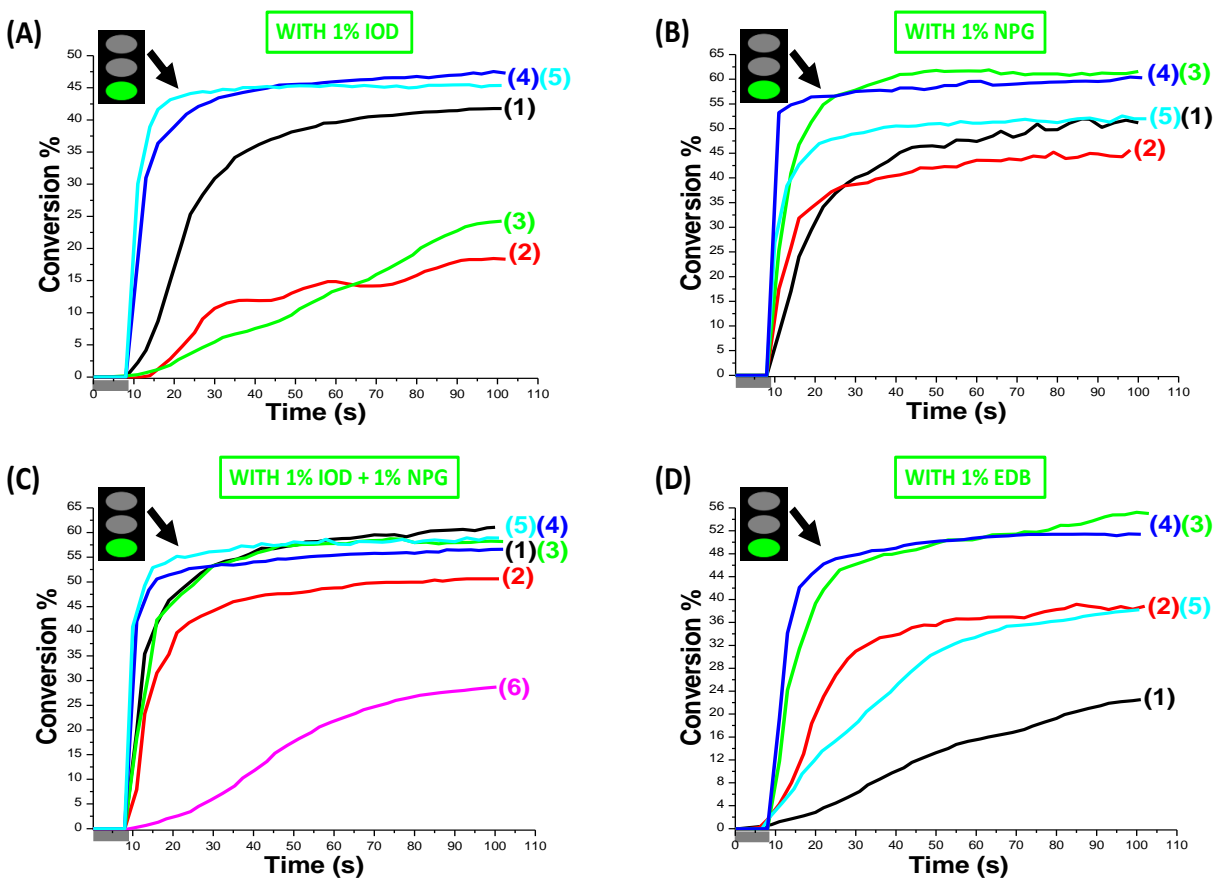


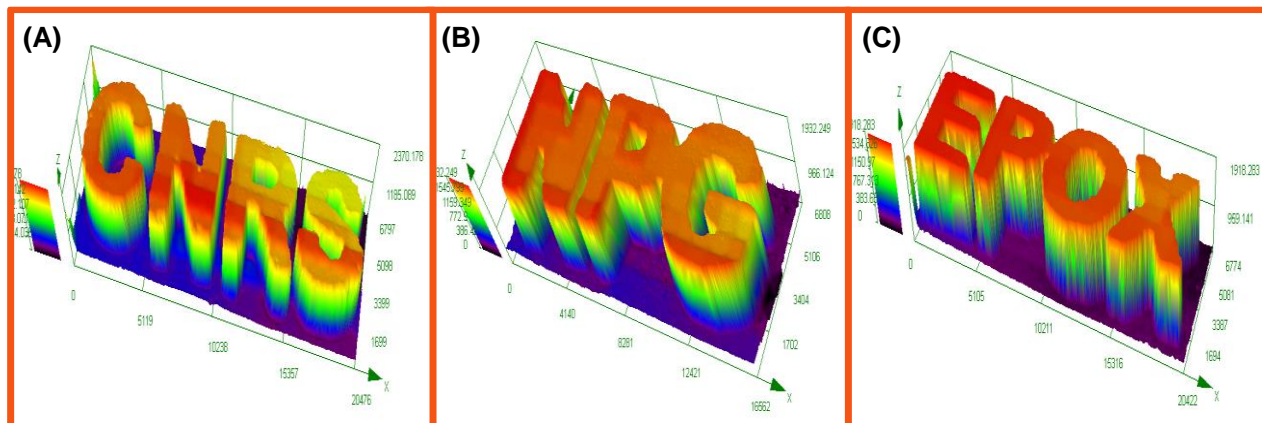
Table 3. Final Reactive Acrylate Function Conversion (FC) for TMPTA in the Presence of Different Two (0.5%/1% w/w) and Three-Component (0.5%/1%/1% w/w) PISs after 100 s of Irradiation with the LED @405 nm.

	Dye/Iod	Dye/NPG	Dye/EDB	Dye/Iod/NPG
Dye 1	42%	52%	23%	62%
Dye 2	19%	46%	39%	51%
Dye 3	25%	62%	55%	59%
Dye 4	48%	61%	52%	57%
Dye 5	46%	53%	39%	60%

3.5. 3D Printing Experiments

3D printing experiments were performed in order to obtain 3D patterns in the presence of different Dye/Additive combinations. The 3D patterns were generated under air by means of a laser diode (@405 nm). Laser write experiments were successfully performed in the presence of **Dye 2/Iod/DPPBA**, **Dye 4/NPG** or **Dye 4/Iod PISs** using acrylates (TMPTA) or TMPTA/EPOX mixture as organic resins. DPPBA was used as the additive to overcome the oxygen inhibition. Thick 3D polymer samples (with very high spatial resolution) were obtained in a very short time of irradiation (< 1 min). Actually, the spatial resolution is only limited by the size of the laser diode beam (50 μm). Numerical optical microscopy was used to characterize the 3D patterns (Figure 6).

Figure 6. Laser write experiments (@405 nm): Characterization of the 3D patterns by a numerical optical microscopy: (A) **Dye 2/Iod/DPPBA** (0.05%/0.1%/0.1% w/w) in TMPTA (thickness = 2370 μm), (B) **Dye 4/NPG** (0.043%/0.087% w/w) in TMPTA (thickness = 1930 μm), and (C) **Dye 4/Iod** (0.0625%/0.125% w/w) (thickness = 1920 μm); respectively.



3.6. Near-UV Conveyor Experiments for the Preparation of Photocomposites

The photocomposites were prepared by the impregnation of glass fibers by an organic resin (50% glass fibers/50% resin w/w) where TMPTA was used as the organic monomer in this study. The prepared prepreps were irradiated with a LED@395 nm. Photos before and after irradiation have been taken (Table 4). A very fast curing was observed in the presence of the investigated

dyes where a single pass of irradiation was enough for the surface to become tack-free (for 2 m/min belt speed) and few passes for the bottom of the sample, using one layer of glass fibers (thickness = 2 mm). The results obtained are summarized in Table 4. Therefore, the investigated dyes presented a remarkable reactivity for the production of photocomposite materials with an excellent depth of cure.

Table 4. Photocomposites produced upon Near-UV light (LED@395 nm), Belt Speed = 2 m/min, for free radical polymerization (FRP) in the presence of glass fibers/acrylate resin (50%/50% w/w) (thickness = 2 mm for one layer of glass fibers) using different systems: (1) 0.5% **Dye 2** + 1% EDB in TMPTA; and (2) 0.5% **Dye 4** + 1% NPG in TMPTA.

Photoinitiating Systems in TMPTA	Before Irradiation	After Irradiation with the LED at 395 nm	Number of Passes at The Surface to Become Tack-free	Number of Passes for The Bottom to Become Tack-free
Dye 2 /EDB (0.5%/1% w/w)			1 Pass	4 Passes
Dye 4 /NPG (0.5%/1% w/w)			1 Pass	5 Passes

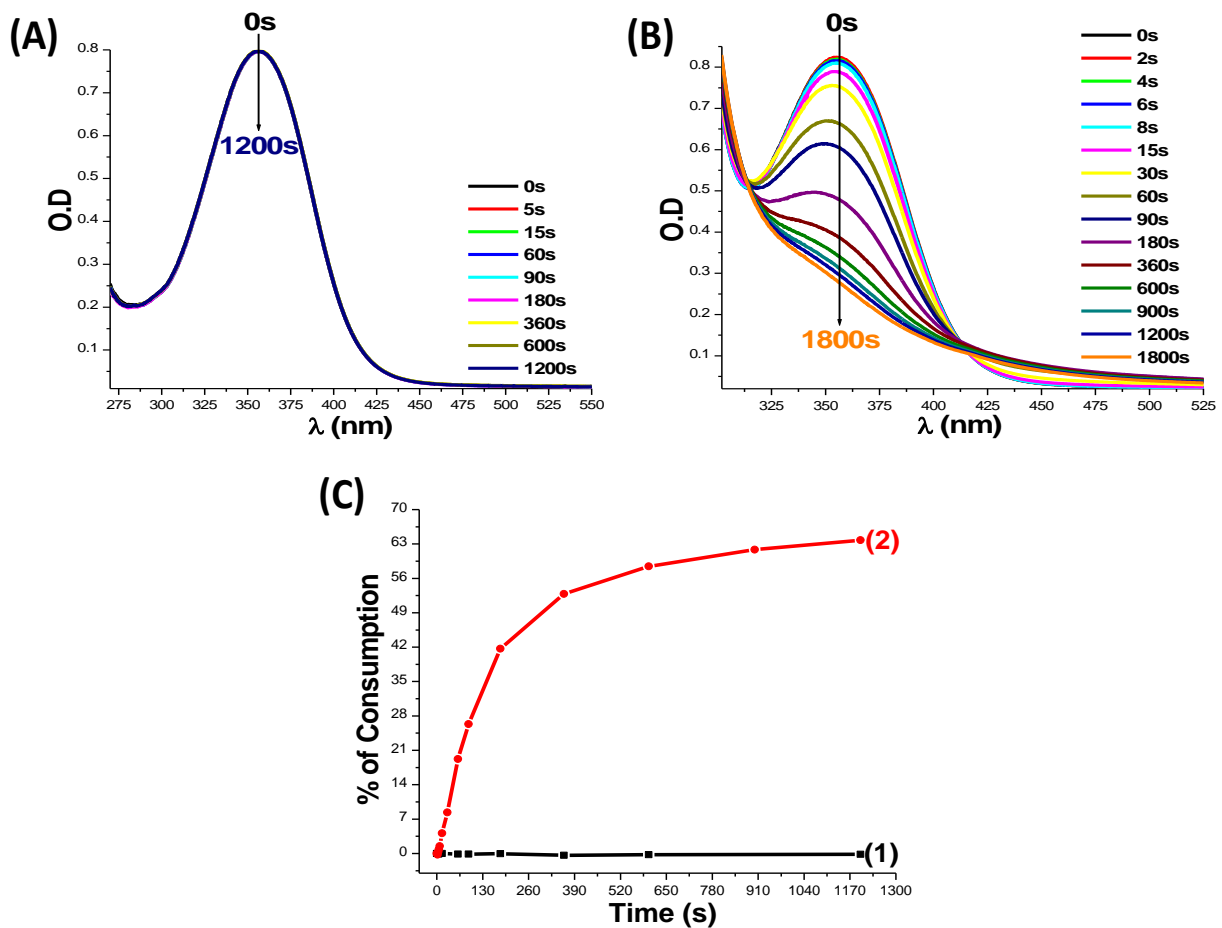
3.7. Chemical Mechanisms

3.7.1. Steady State Photolysis

The steady state photolysis experiments for the investigated dyes were performed in acetonitrile using a UV-visible spectroscopy. Obviously, a very fast photolysis was observed for **Dye 4** in the presence of the iodonium salt when the (**Dye 4**/Iod) solution was irradiated with the LED@375 nm compared to the very high photostability of **Dye 4** alone where no photolysis occurs (Figure 7B vs. Figure 7A, respectively), suggesting a strong interaction between **Dye 4** and

Iodonium salt. Indeed, an isobestic point arises at about 315 nm showing that no other secondary reaction occurs. The percentage of consumption of **Dye 4** in the presence of Iod (curve 2) or without Iod (curve 1) are presented in Figure 7C at different **times** of irradiation i.e. % of consumption_(max) = 64% after **200 s** of irradiation in the presence of Iod compared to the non-consumption for **Dye 4** alone. Very fast **photolyses** were also obtained for **Dye 1**, **Dye 3** or **Dye 5** in the presence of Iod compared, while almost no photolysis occurs for **Dye 2**/Iod and **Dye 2** alone. On the other hand, no or very low photolysis in the presence of NPG or EDB was observed for the investigated dyes (except for **Dye 1**/EDB where a fast photolysis was observed), showing that there is perhaps a back electron transfer reaction when using amine as co-initiator.

Figure 7. (A) Photolysis of **Dye 4** alone in ACN; (B) **Dye 4**/Iod photolysis in ACN; and (C) % of Consumption of **Dye 4** without (1) and with (2) Iodonium salt vs. Irradiation time using the LED @375 nm.



3.7.2. Proposed Photochemical Mechanisms Based on Fluorescence Quenching, Cyclic Voltammetry and ESR Experiments

The values of the singlet excited state energy for the examined dyes are determined from the crossing point between the absorption and the fluorescence spectra e.g. $E_{S1} = 2.89$ eV for **Dye 4** (See Table 5). The fluorescence and fluorescence quenching experiments were carried out in acetonitrile (Figure 8). For **Dye 1** and **Dye 3**, no fluorescence is observed in acetonitrile.

Figure 8. (A) Singlet state energy determination for **Dye 4** in acetonitrile; and (B) Fluorescence quenching of **Dye 4** by Iod.

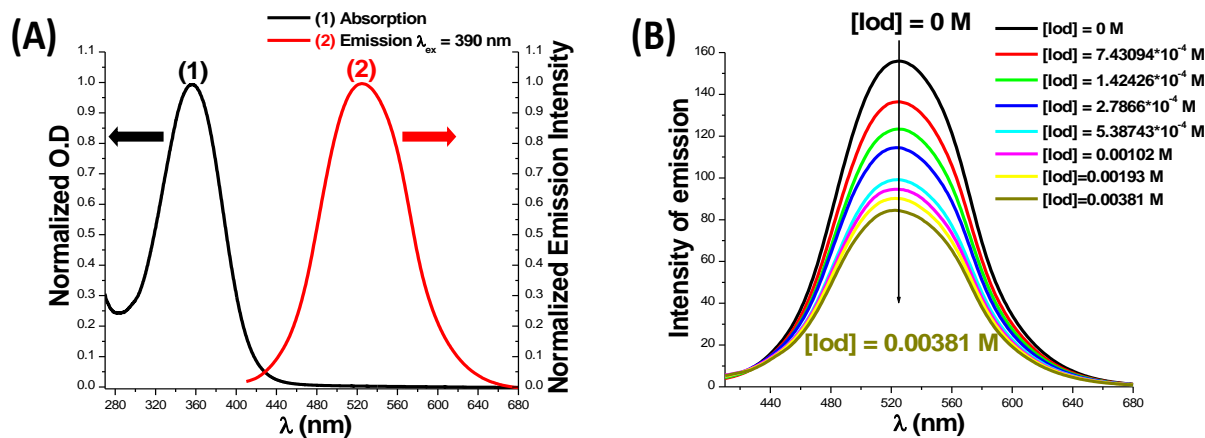


Table 5. Parameters Characterizing the Photochemical Mechanisms Associated with $^{1,3}\text{Dye/Iod}$, $^{1,3}\text{Dye/NPG}$ and $^{1,3}\text{Dye/EDB}$ in Acetonitrile.

	E_{S1} (eV)	E_{T1} (eV) ^a	E_{ox} (eV)	$\Delta G_{et(S1)}^b$ $^1_{(PI/Iod)}$ (eV)	$\Delta G_{et(T1)}^b$ $^3_{(PI/Iod)}$ (eV)	E_{red} (eV)	$\Delta G_{et(S1)}^c$ $^1_{(PI/Amine)}$ (eV)	$\Delta G_{et(T1)}^c$ $^3_{(PI/Amine)}$ (eV)	K_{SV} (PI/Iod) (M^{-1})	$\phi_{et(S1)}^d$ (PI/Iod)	K_{SV} (PI/NPG) (M^{-1})	$\phi_{et(S1)}^d$ (PI/NPG)	K_{SV} (PI/EDB) (M^{-1})	$\phi_{et(S1)}^d$ (PI/EDB)
Dye 1	2.46	2.08	1.08	-1.18	-0.8	-1.66	0.3	0.68	-	-	-	-	-	-
Dye 2	2.71	2.06	0.46	-2.05	-1.4	-1.25	-0.36	-0.25	37	0.41	40	0.73	86	0.82
Dye 3	3.03	2.6	1.06	-1.77	-1.34	-1.45	-0.48	-0.05	-	-	-	-	-	-
Dye 4	2.89	2.6	1.01	-1.68	-1.39	-1.4	-0.39	-0.1	188	0.78	102	0.87	50	0.72
Dye 5	2.92	2.18	0.81	-1.91	-1.17	-1.44	-0.38	0.36	60	0.53	40	0.73	256	0.93

a: calculated triplet state energy level at DFT level.

b: for Iod, a reduction potential of -0.2 eV was used for the $\Delta G_{et}^{1,3}(\text{Dye/Iod})$ calculations [3].

c: for Amine, an oxidation potential of 1.1 eV was used for the $\Delta G_{et}^{1,3}(\text{Dye/Amine})$ calculations [3].

d: from the eq. 2 presented in [3].

Favorable fluorescence quenching processes were observed for **¹Dye 2** (or **Dye 4** or **Dye 5**)/Iod with high values of the Stern-Volmer coefficients (**K_{sv}**; Table 5) and also high values of the electron transfer quantum yield (**φ_{et}**; calculated according to eq. 2; Table 5). These results are in full agreement with the highly favorable free energy changes (**ΔG_{et(Dye/Iod)}**) for the electron transfer reaction which takes place between dyes and Iod (r1 and r2 in Scheme 3). This latter was calculated according to the equation 1 where the oxidation potentials (**E_{ox}**) of the different dyes are determined by cyclic voltammetry experiments (Table 5).

$$\phi_{et} = K_{sv}[Iod]/(1+K_{sv}[Iod]) \quad (\text{eq 2})$$

A triplet state pathway cannot be fully excluded with favorable values of the free energy change (**ΔG_{et(T1)}**) for **³Dye**/Iod (Table 5). But, the singlet pathway has a preponderance over the triplet one due to very high electron transfer quantum yields.

Otherwise, the values of the free energy changes (**ΔG_{et(S1 or T1)}**) for the electron transfer reaction **^{1,3}Dye**/Amine are also given in Table 5 where the reduction potentials of the different examined dyes are determined from cyclic voltammetry experiments (e.g. for **Dye 3**, **E_{red}** = -1.45 V; Table 5).

According to other reported photoinitiating systems [40,41], a global photochemical mechanism is proposed in Scheme 3 (reactions r1-r8). For the photo-oxidation process, the interaction between dyes as electron donors and Iod as electron acceptor leads to the generation of aryl radicals (**Ar[•]**). This latter interaction is confirmed by ESR experiments that are able to detect the generated aryl radicals under the form of (PBN/**Ar[•]**) radical adducts in the Dye/Iod irradiated solution [3]. Actually, (PBN/**Ar[•]**) radical adducts are characterized by typical hyperfine coupling constants (hfcs): **a_N** = 14.1 G and **a_H** = 2.1 G in full agreement with reported data [42]. As reported

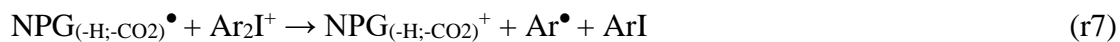
in [3], aryl radicals are considered among the most efficient initiating species for the addition onto methacrylate double bond ($k_{\text{add}} \sim 10^8 \text{ M}^{-1} \cdot \text{s}^{-1}$) [9] which is in full agreement with the high reactivity showed by the Dye/Iod couples.

Based on recently published data [43], the formation of a Charge Transfer Complex (CTC) between NPG (*N*-aromatic electron donor) and iodonium salt (electron poor) can be also suggested (r3). This complex is able to provide an enhanced visible light absorption to the photoinitiating system resulting in a better reactivity. This behavior is confirmed by the photopolymerization study (curve 6 in Figure 5C) where the photolysis of this latter structure at 405 nm leads to an efficient release of aryl radicals Ar^\bullet (r4).

Besides, an electron/proton transfer reaction can be proposed (r1 and r5) for the Dye/amine couples. Then, a decarboxylation reaction (r6) is suggested for NPG in order to avoid any back electron transfer reaction [3]. Therefore, $(\text{NPG}_{(-\text{H};-\text{CO}_2)})^\bullet$ can be considered as the initiating species for the FRP in the presence of Dye/NPG systems.

Furthermore, r7 and r8 are proposed for the interactions that occurs in the presence of the three-component systems (Dye/Iodonium salt/Amine combinations) [43]. As a result, Ar^\bullet , $\text{NPG}_{(-\text{H};-\text{CO}_2)}^\bullet$, and $\text{Dye}^{\bullet+}$ can be considered as the initiating species for the FRP and the CP, respectively.





Scheme 3. Proposed Photochemical Mechanisms.

Conclusion:

In summary, high performance dyes based on triphenylamine, cinnamaldehyde and 1,3-indanedione derivatives have been synthesized and examined as excellent visible light photoinitiators for photopolymerization processes. Both the cationic polymerization of thin epoxide samples and the free radical polymerization of thin acrylate films were performed upon irradiation with the LED at 405 nm. The investigated dyes exhibited very high efficiencies in terms of final reactive function conversions (FCs) and also rates of polymerization (R_p) due to their high extinction coefficients in the near-UV and blue region, their suitable oxidation potentials and free energy changes. These dyes also showed a high reactivity in 3D printing experiments. The production of thick glass fiber photocomposites has been well accomplished. Future development of new co-initiators able to increase the reactivity of the initiating systems are ongoing and will be presented in our upcoming works.

ACKNOWLEDGMENTS

The Lebanese group would like to thank “The Association of Specialization and Scientific Guidance” (Beirut, Lebanon) for funding and supporting this scientific work.

REFERENCES

- [1] Fouassier J.P.; Allonas X.; Burget D. Photopolymerization reactions under visible lights: principle, mechanisms and examples of applications. *Prog. Org. Coat.* **2003**, 47, 16-36.
- [2] Fouassier J.P. Photoinitiator, Photopolymerization and Photocuring: Fundamentals and Applications; Gardner Publications: New York. **1995**.
- [3] Fouassier J.P.; Lalevée J. Photoinitiators for Polymer Synthesis, Scope, Reactivity, and Efficiency; Wiley-VCH Verlag: Weinheim, Germany. **2012**.
- [4] Dietliker K. A Compilation of Photoinitiators Commercially Available for UV Today; Sita Technology Ltd.: London. **2002**.
- [5] Davidson S. Exploring the Science, Technology and Application of UV and EB Curing; Sita Technology Ltd.: London. **1999**.
- [6] Crivello J.V.; Dietliker K.; Bradley G. Photoinitiators for Free Radical Cationic & Anionic Photopolymerisation; John Wiley & Sons: Chichester, U.K. **1999**.
- [7] Green W. A. Industrial Photoinitiators: A Technical Guide, CRC Press. **2010**.
- [8] Kahveci M.U.; Yilmaz A.G.; Yagci Y. in Photochemistry and Photophysics of Polymer Materials, ed. N. S. Allen, John Wiley & Sons, Inc. **2010**, 421-478.
- [9] Strehmel B.; Brömme T.; Schmitz C.; Reiner K.; Ernst S.; Keil D. in Dyes and Chromophores in Polymer Science, Ed. Lalevée J.; Fouassier J.P. John Wiley & Sons, Inc. **2015**, 213-249.
- [10] Yagci Y.; Jockusch S.; Turro N.J. Photoinitiated Polymerization: Advances, Challenges, and Opportunities. *Macromolecules*, **2010**, 43, 6245-6260.

- [11] Lalevée J.; Fouassier J.P. in *Dye Photosensitized Polymerization Reactions: Novel Perspectives*, RSC Photochemistry Reports, Ed. A. Albini and E. Fasani, Photochemistry, London, UK. **2015**, 215-232.
- [12] Vallo C. I.; Asmussen S. V. In *Photocured Materials*; Tiwari A.; Polykarpov A. Eds.; RSC Smart Materials Series 13; The Royal Society of Chemistry: Cambridge. **2015**, 321-346.
- [13] Abdallah M.; Bui T.T.; Goubard F.; Theodosopoulou D.; Dumur F.; Hijazi A.; Fouassier J.P.; Lalevée J. Phenothiazine Derivatives as Photoredox Catalysts for Cationic and Radical Photosensitive Resins for 3D Printing Technology and Photocomposite Synthesis. *Polym. Chem.* **2019**, 10, 6145–6156.
- [14] Crivello J.V. in *Dyes and Chromophores in Polymer Science*, Ed. Lalevée J.; Fouassier J.P. John Wiley & Sons, Inc. **2015**, 45-79.
- [15] Sangermano M.; Razza N.; Crivello J.V. Cationic UV-Curing and Applications. *Macromol. Mater. Eng.* **2014**, 299, 775-793.
- [16] Bongiovanni R.; Sangermano M. in *Encyclopedia of Polymer Science and Technology*, John Wiley & Sons, Inc., Hoboken, NJ, USA. **2014**, 1-20.
- [17] Xiao P.; Dumur F.; Graff B.; Gigmès D.; Fouassier J.P.; Lalevée J. Blue Light Sensitive Dyes for Various Photopolymerization Reactions: Naphthalimide and Naphthalic Anhydride Derivatives. *Macromolecules.* **2014**, 47, 601-608.
- [18] Hsia Chen C. S. Dye-sensitized photopolymerization. I. Polymerization of acrylamide in aqueous solution sensitized by methylene blue–triethanolamine system. *J. Polym. Sci. A Polym. Chem.* **1965**, 3, 1107-1125.

- [19] Zhang J.; Lalevée J.; Zhao J.; Graff B.; Stenzel M. H.; Xiao P. Dihydroxyanthraquinone Derivatives: Natural Dyes as Blue-Light-Sensitive Versatile Photoinitiators of Photopolymerization. *Polym. Chem.* **2016**, *7*, 7316-7324.
- [20] Tehfe M.A.; Dumur F.; Graff B.; Gignes D.; Fouassier J.P.; Lalevée J. Blue-to-Red Light Sensitive Push–Pull Structured Photoinitiators: Indanedione Derivatives for Radical and Cationic Photopolymerization Reactions. *Macromolecules.* **2013**, *46*, 3332-3341.
- [21] Xiao P.; Dumur F.; Graff B.; Morlet-Savary F.; Vidal L.; Gignes D.; Fouassier J.P.; Lalevée J. Structural Effects in the Indanedione Skeleton for the Design of Low Intensity 300–500 nm Light Sensitive Initiators. *Macromolecules.* **2014**, *47*, 26-34.
- [22] Zhou T. F.; Ma X. Y.; Han W. X.; Guo X. P.; Gu R. Q.; Yu L. J.; Li J.; Zhaoc Y. M.; Wang T. D-D-A dyes with phenothiazine-carbazole/triphenylamine as double donors in photopolymerization under 455 nm and 532 nm laser beams. *Polym. Chem.* **2016**, *7*, 5039-5049.
- [23] Li Y.H.; Chen Y.C. Triphenylamine-hexaarylbiimidazole derivatives as hydrogen-acceptor photoinitiators for free radical photopolymerization under UV and LED light. *Polym. Chem.* **2020**, under press.
- [24] Tomeckova V.; Norton S. J.; Love B. J.; Halloran J. W. Photopolymerization of acrylate suspensions with visible dyes. *J. Eur. Ceram.* **2013**, *33*, 699-707.
- [25] Fouassier J.P.; Morlet-Savary F.; Lalevée J.; Allonas X.; Ley C. Dyes as Photoinitiators or Photosensitizers of Polymerization Reactions. *Materials.* **2010**, *3*, 5130-5142.
- [26] Tehfe, M.-A.; Dumur, F.; Graff, B.; Morlet-Savary, F.; Gignes, D.; Fouassier, J.-P.; Lalevée, J. Push–pull (thio)barbituric acid derivatives in dye photosensitized radical and cationic

polymerization reactions under 457/473 nm laser beams or blue LEDs, *Polym. Chem.* **2013**, 4, 3866-3875.

[27] Singh, A.; Lim, C.K.; Lee, Y.D.; Maeng, J.-H.; Lee, S.; Koh, J.; Kim, S. Tuning solid-state fluorescence to the near-infrared: a combinatorial approach to discovering molecular nanoprobe for biomedical imaging, *ACS Appl. Mater. Interf.* **2013**, 5, 8881-8888.

[28] Burckstummer, H.; Tulyakova, E.V.; Deppisch, M.; Lenze, M.R.; Kronenberg, N.M.; Gsunger, M.; Stolte, M.; Meerholz, K.; Wurthner, F. Efficient solution-processed bulk heterojunction solar cells by antiparallel supramolecular arrangement of dipolar donor-acceptor dyes, *Angew. Chem. Int. Ed.* **2011**, 50, 11628-11632.

[29] Malina, I.; Kampars, V.; Turovska, B.; Belyakov, S. Novel green-yellow-orange-red light emitting donor-p-acceptor type dyes based on 1,3-indandione and dimedone moieties, *Dyes Pigm.* **2017**, 139, 820-830.

[30] Abdellah, I.M.; Koraiem, A.I.; El-Shafei, A. Molecular engineering and investigation of new efficient photosensitizers/co-sensitizers based on bulky donor enriched with EDOT for DSSCs, *Dyes Pigm.* **2019**, 164, 244-256.

[31] Dheepika, R.; Sonalin, S.; Imran, P.M.; Nagarajan, S. Unsymmetrical starburst triarylamine: synthesis, properties, and characteristics of OFETs, *J. Mater. Chem. C* **2018**, 6, 6916-6919.

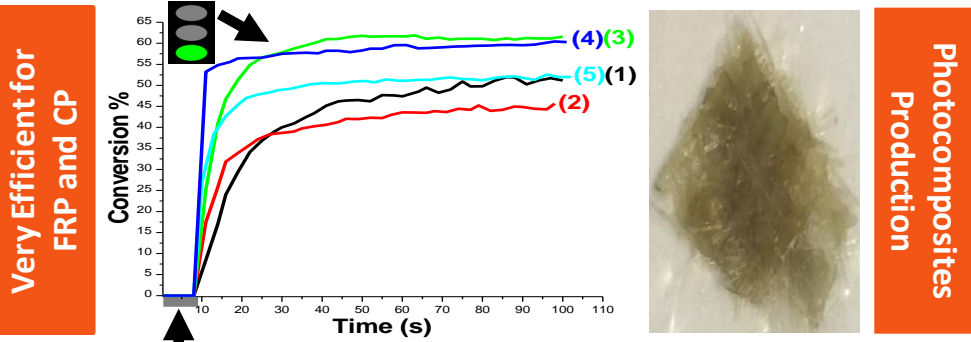
[32] Dietlin C.; Schweizer S.; Xiao P.; Zhang J.; Morlet-Savary F.; Graff B.; Fouassier J.P.; Lalevée J. Photopolymerization upon LEDs: new photoinitiating systems and strategies. *Polym. Chem.* **2015**, 6, 3895-3912.

- [33] Lalevée J.; Blanchard N.; Tehfe M. A.; Morlet-Savary F.; Fouassier J.P. Green Bulb Light Source Induced Epoxy Cationic Polymerization under Air Using Tris(2,2'-bipyridine)ruthenium(II) and Silyl Radicals. *Macromolecules* **2010**, 43, 10191–10195.
- [34] Lalevée J.; Blanchard N.; Tehfe M. A.; Peter M.; Morlet-Savary F.; Gigmes D.; Fouassier J.P. Efficient Dual Radical/Cationic Photoinitiator under Visible Light: A New Concept. *Polym. Chem.* **2011**, 2, 1986–1991.
- [35] Rehm D.; Weller A. A. Kinetics of Fluorescence Quenching by Electron and H-Atom Transfer. *Isr. J. Chem.* **1970**, 8, 259–271.
- [36] Abdallah M.; Le H.; Hijazi A.; Schmitt M.; Graff B.; Dumur F.; Bui T.T.; Goubard F.; Fouassier J.P.; Lalevée J. Acridone derivatives as high performance visible light photoinitiators for cationic and radical photosensitive resins for 3D printing technology and for low migration photopolymer property. *Polym.* **2018**, 159, 47-58.
- [37] Zhang J.; Dumur F.; Xiao P.; Graff B.; Bardelang D.; Gigmes D.; Fouassier J.P.; Lalevée J. Structure Design of Naphthalimide Derivatives: Toward Versatile Photoinitiators for Near-UV/Visible LEDs, 3D Printing, and Water-Soluble Photoinitiating Systems. *Macromolecules* **2015**, 48, 2054–2063.
- [38] Xiao P.; Dumur F.; Zhang J.; Fouassier J.P.; Gigmes D.; Lalevée J. Copper Complexes in Radical Photoinitiating Systems: Applications to Free Radical and Cationic Polymerization upon Visible LEDs. *Macromolecules* **2014**, 47, 3837–3844.
- [39] Budreckiene R.; Lazauskaite R.; Buika G.; Grazulevicius J.V. Cationic photopolymerization of carbazolyl-containing vinyl ethers. *J. Photochem. and Photobio. A Chem.* **2003**, 157, 117-123.

- [40] Abdallah M.; Hijazi A.; Graff B.; Fouassier J.P.; Rodeghiero G.; Gualandi A.; Dumur F.; Cozzi P.G.; Lalevée J. Coumarin Derivatives as Versatile Photoinitiators for 3D Printing, Polymerization in Water and Photocomposite Synthesis. *Polym. Chem.* **2019**, 10, 872–884.
- [41] Zivic N.; Bouzrati-Zerelli M.; Kermagoret A.; Dumur F.; Fouassier J.P.; Gignes D.; Lalevée J. Photocatalysts in Polymerization Reactions. *ChemCatChem* **2016**, 8, 1617–1631.
- [42] Lalevée J.; Fouassier J.P. Dyes and Chromophores in Polymer Science, Wiley-ISTE, London, **2016**.
- [43] Garra P.; Graff B.; Morlet-Savary F.; Dietlin C.; Becht J.M.; Fouassier J.P.; Lalevée J. Charge Transfer Complexes as Pan-Scaled Photoinitiating Systems: From 50 μm 3D Printed Polymers at 405 nm to Extremely Deep Photopolymerization (31 cm). *Macromolecules* **2018**, 51, 57–70.

TOC Graphic:

High Performance Dyes Based on Triphenylamine, Cinnamaldehyde and Indane-1,3-dione Derivatives for Blue Light Induced Polymerization for 3D Printing and Photocomposites



3D Printing Technology

